A lab approach to Simulate the Effects of Thermoforming on the Gas Permeability of Commercial Multilayers

[1,2]Buntinx Mieke*, [1,2]Dimitri Adons, [2]Liam Reekmans, [2]Tuur Bollen, [2]Jill Raemaekers, [2]Dries Hermans, [2]Evelynn Vervoort, [2]Quinten Poulisse, [2]Gwen Duijsters and [1,2]Roos Peeters

[1] *Hasselt University, Materials and Packaging Research & Services (MPR&S), Institute for Materials Research (imo-imomec), Wetenschapspark 27, Diepenbeek, Belgium;*
[2] *Faculty of Engineering Technology, University Campus, Diepenbeek, Belgium*

**Corresponding author. Email: mieke.buntinx@uhasselt.be*

Abstract: In the search for sustainable food packaging, critical reflection on the choice, combination and quantity of (bio)materials for specific applications is becoming increasingly important to prevent food waste. Our previous research has shown the combined effects of material thinning and polymer reorientation on the gas permeability of thermoformed multilayer trays. This study aims to investigate the feasibility of simulating the thermoforming process by heating and deforming (bio)plastic multilayers in a lab scale set-up to determine the maximum thinning and the associated gas permeability properties.

First, thermal and tensile properties of commercial PE/EVOH/PE and ecovio®/G-Polymer/ecovio multilayer films (~85 µm) are characterized. Next, tensile testing at selected temperatures is applied to determine the maximum stretch, based on the elongation at break. Then, hot stretching of 70x60 mm^2-films in machine and/or cross direction (MD, CD, MD+CD) or 45°, is done in an oven at optimal temperature by applying maximum gravity without breaking the multilayer. The microscopical thickness resulting from these situations is compared with the thinning in the bottom, walls and corners of thermoformed trays. The results show that thinning of both films is proportional to an increase in the water vapor transmission rate (WVTR), with the PE-layers providing a better water vapor barrier than the ecovio-layers. In contrast, the oxygen transmission rate (OTR) is not proportional to thinning of the total film, nor the thickness of the barrier layer. Here, polymer reorientation comes into play, even resulting in improved oxygen permeability coefficients as compared to the base films.

We conclude that this approach can support the optimization of thermoforming processes by determining the maximal stretch of the individual layers while safeguarding the gas barrier properties of the final packaging, e.g. in thermoformed fiber-based trays.

Keywords: thermoforming, multilayer food packaging, OTR, WVTR, oxygen barrier, water vapor barrier.

1 Introduction

In the search for **sustainable** food packaging that prevent food waste, the selection, combination and quantity of (bio)materials for specific applications is crucial. In addition to functionality and eco-friendly material-use, sustainable packaging should also consider the best possible end-of-life option, as well as efficient technical performance during processing.

Multilayer packaging materials are still considered highly efficient and environmental beneficial solutions when compared to alternatives, due to the sophisticated balance between mechanical performance necessary for logistics and handling, thermal stability required for filling and/or thermal treatment, optics for customer appeal, sealability for closure, gas, water or aroma barrier properties needed for content preservation and lightweight design, enabling resource reduction [1].

However, at the end-of-life, multilayer packaging is currently predominantly incinerated, as they cannot be recycled in the existing waste management infrastructure that rely on traditional mechanical recycling [2]. This contradicts the core principles of a circular economy, particularly within the European Union (EU), where plastic packaging stands as a top priority within circularity initiatives. With plastic packaging waste recycling reaching only 39.6% in 2021 [3], the imperative for circularity is intensified by the upcoming enactment of the Packaging and Packaging Waste Regulation [4], setting a 55% recycling target for plastic packaging by 2030.

To comply with the new regulation, design for recycling aims to reduce the multilayer complexity. However, when a less complex mono-material solution shows better recyclability, but is associated with higher material input or shorter shelf life compared to a multilayer solution, it is neither environmental favorable [5].

Nowadays, there is a shift towards minimizing multilayer material diversity, primarily favoring polyolefins, and tolerating ethylene vinyl alcohol copolymer (EVOH), metallized aluminum layers, and aluminum oxide (AlOx) or silicon oxide (SiOx) coatings to a certain extent to enhance the barrier properties. To meet recycling standards outlined by Ceflex or RecyClass guidelines, multilayers must consist of a least 90% polyolefin content to qualify as mono-material suitable for recycling. Coextrusion or lamination with EVOH is preferable over AlOx and SiOx, as these coatings are generally not suitable for sterilizable packaging nor deep draw applications [2]. RecyClass recyclability testing shows that EVOH has a minor impact on the recycled material at a threshold of up to 5% of the total weight of the PE film. Above this limit, immediate impact on the extrusion process is observed resulting in yellowing of the material, an increase of haze and gels and black specks, and a frequent bubble breakage [6].

Another way to meet circularity for multilayers involves better recycling technologies. In the near future, a mix of distinct recycling technologies (e.g. high-performance material recycling, chemical recycling into hydrocarbons, and downcycling) will develop in different parts of the world. This evolution will strongly depend on local regulations and technology availability [7].

However, even if developed countries have the most efficient technology to recycle multilayers, a great part of the world will still lack basic waste management and conventional recycling systems. Therefore, the use of biobased materials in multilayers is still suggested as a short-term opportunity to reduce carbon emission and decouple packaging materials from the fossil-based economy [8]. Moreover, biodegradable food packaging, which is often contaminated with food can be disposed of together with food waste, and further processed through composting or organic material recycling. Moreover, biodegradable films offer better compatibility with compostable fiber-based materials and are ideal suited for paper lining.

Thus, pending better recycling technologies and infrastructure (collection, sorting, recycling), two strategies for minimizing the environmental impact of multilayers seem best feasible: i) reduction in the amount of material used (thinner packaging) and/or, ii) use of biobased and biodegradable materials. Nonetheless, ensuring mechanical and barrier performance with regard to the packed product, particularly after material processing, remains a primary concern. Our previous research has shown the combined effects of material thinning and potential polymer reorientation on the gas permeability of thermoformed multilayer trays [9, 10]. This study aims to investigate the feasibility of simulating the thermoforming process by heating and deforming multilayers in a lab scale set-up to determine the maximum thinning and the associated mechanical and gas permeability properties of commercial PE/EVOH/PE and Ecovio®/G-polymer/Ecovio multilayers.

2 Materials and methods

2.1 Materials

Two commercial multilayer films (~85 µm) were studied: i) PE/EVOH/PE and ii) Ecovio®/G-Polymer/Ecovio. The material composition of each multilayer was confirmed based on the typical melt and crystallisation temperatures identified in Differential Scanning Calorimetry analysis (*DSC data not shown*).

2.2 Material characterization

2.2.1 Total and individual layer thickness measurements before and after stretching

Total film thickness was measured using an MTS Micrometer (MTS systems, France) (n=3-10).

Total and individual layer thickness of original and stretched films and in selected locations of thermoformed trays was determined using a Nikon Eclipse ME600 Microscope equipped with Nikon DS-Fi2 camera (Nikon, Tokyo, Japan) and NIS Elements software. A small strip (4 mm x 30 mm) was cut from the film or tray, folded in half and positioned in a calliper, extending several millimetres above it. The protruding sample was then trimmed at an angle of 45° using a sharp knife. Next, the calliper was placed under the microscope and the thickness of the individual layers was determined. Iodine was used to stain the EVOH layer yellow in the PE/EVOH/PE film to identify it more easily [11].

The percentage of thinning was calculated using equation 1, with d_0 and d_s representing the average thickness of the original film and the stretched film, respectively.

$$thinning\ (\%) = \frac{d_0 - d_s}{d_0} \times 100\% \tag{1}$$

Total thickness of films and trays was also measured by means of a handheld thickness gauge (Magna-Mike 8600, Olympus NDT Inc., Aartselaar, Belgium). A grid of squares of ~1 cm² was drawn on the trays and the thickness was measured in the squares, as described earlier [9, 10]. The percentage of thinning was calculated in every square ('i') according to equation 2, with d_0 and d_i representing the thickness of the film and the thickness in square 'i', respectively.

$$thinning\ (\%) = \frac{d_0 - d_i}{d_0} \times 100\% \qquad (2)$$

The average measured thickness of the trays was calculated according to equation 3 in which A_i and d_i represent the area and thickness of square 'i' respectively:

$$d_{average}(\mu m) = \frac{\sum_{i=1}^{n}(d_i \cdot A_i)}{\sum_{i=1}^{n} A_i} \qquad (3)$$

2.2.2 Tensile testing

Rectangular film samples (15 mm x 40 mm) were tested at 23°C, 50°C, 75°C, 90°C and 120°C, both in machine direction (MD) and cross direction (CD), to determine the tensile stress at break (σ_b, in MPa), maximal force at break (F, in N) and elongation at break (ε, in %). The tests were performed in triplicate using a climatized tensile tester (Tinius Olsen Bench Mounted ST Series) with following settings: 2 min conditioning at the set temperature, distance of the film between the clamps of 20 mm, preload of 0.20 N, and speed of 500 mm·min^{-1}.

2.3 Methods to simulate thermoforming at lab scale

2.3.1 Hot stretching using gravimetrical force

A metal construction with a total mass of 155 g and a height of 23 cm was assembled to fix and subsequently stretch a clamped film by attaching a specific mass to the sample holder (**Figure 1**) in a heated oven.

Film samples (70 mm x 60 mm) were clamped between aluminium plates (30 x 120 mm) and conditioned for 2 min at 120°C in an oven (Heraeus Thermicon P, Germany). Next, masses of 640 to 3000 g were added to the sample holder based on the material's measured maximal force at break (in the tensile tests). Hot stretching using gravity was done at temperatures between 100-120°C. This procedure was optimized for maximal strain without breaking the film.

Figure 1: Self-made metal construction to stretch multilayer films using gravity in an oven.

2.3.2 Thermoforming using a lab thermoformer

To simulate a vacuum forming process on lab scale, different moulds made from a quick casting resin PUR MC5 (Vosschemie, Benelux) were fabricated using 3D-printed polylactic acid (PLA) negative moulds and finished off by milling the edges and drilling holes to allow airflow for vacuum forming. The moulds were subsequently used in the Formech 450 DT thermoformer (MakerSpace, UHasselt) to produce trays with different dimensions of length (L), width (W) and height (H), and different total tray areas (**Table 1**). The quartz heaters were preheated for 15 min at 40% heating capacity, generating 115°C, before vacuum forming the multilayers.

Table 1: Overview of thermoformed trays with dimensions, total tray area and OTR or WVTR when measured.

Tray type	PE/EVOH/PE	Eco/G-Pol/Eco	L x W x H	Tray area	OTR	WVTR
A			17.1 cm x 12.3 cm x 2.0 cm	280 cm^2	✶	
B			14.0 cm x 9.0 cm x 4.0 cm	326 cm^2	✶	✶
C			18.3 cm x 13.5 cm x 4.0 cm	394 cm^2	✶	
D			19.4 cm x 14.6 cm x 6.0 cm	691 cm^2		

2.4 Oxygen transmission rate (OTR) measurements

The OTR was measured using MOCON Ox-Tran SL, MH or 702 modules.

The OTR of the original and stretched films was measured according to ASTM F-1927 [12] at 23°C and controlled relative humidity (RH). Flat film samples were clamped in the diffusion cell, which was purged of residual oxygen using an oxygen-free carrier gas (formier). Then pure oxygen (99.9995%) was introduced in the outside chamber of the diffusion cell (50% RH) and the oxygen molecules permeating through the film to the inside chamber (90% RH) were conveyed to the sensor by the humidified carrier gas. The original films were measured in duplicate, with a test area of 50 cm^2. The stretched films were measured once using a mask with test area of 3.7-4.0 cm^2. The OTR was calculated by normalizing the flow rate at steady state with respect to the oxygen pressure gradient and expressed in cc/[m^2·day·atm].

The OTR of the original films and thermoformed trays was measured according to ASTM F-1307 [13] at 23°C with 50% RH outside and 50% RH inside the package. The topside of the tray was sealed with an impermeable adhesive on a copper plate, which was provided with 2 holes for connection to the copper tubings with inflow and outflow of the carrier gas to the Mocon Ox-Tran. The trays were exposed to normal air (20.9% O_2) and the oxygen permeation was measured from the outside to the inside of the tray. The OTR of the trays is recalculated into units of 100% O_2 (expressed in cc/[package·day·atm]). By dividing this OTR by the tray surface, the OTR of the trays can also be expressed in cc/[m^2·day·atm]. All trays were measured once or twice.

In this study, the oxygen permeability coefficient (PO_2) is calculated by normalizing the OTR for the thickness of the barrier layer (EVOH or G-polymer).

2.5 Water vapor transmission rate (WVTR) measurements

The WVTR was determined using Mocon Perma-tran -W, MG, SW or 700 modules and a cup test.

The WVTR of the original and stretched films was measured at 23°C according to ASTM Standard F-1249 [14] with a RH of 50% outside and 0% inside. The original films were measured in duplicate, with a test area of 50 cm^2. The stretched films were measured once using a mask with a final test area of 3.7-4.0 cm^2. WVTR results are expressed in g/[m^2·day] (the consecutively CD+MD stretched films were not measured for WVTR). Additionally, the biofilm was tested in other RH conditions: 37% RH outside/0% inside and 90% RH outside and 0% RH inside.

The WVTR of the trays was also measured at 23°C using a RH gradient of 50% outside to 0% inside, but mostly the detection limit of the Perma-tran SW module (0.1 g/m^2 day) was exceeded. Therefore, tray type B was tested at 25% RH outside and 0% RH inside.

The sensitivity of the multilayers to higher relative humidity was tested via the cup test water method at 23°C according to ASTM E-96. The films (n=4) with exposed area of 32 cm^2 were placed on cups filled with 50 ml water (100% RH inside). The sealed cups were stored in a climatized lab with a RH of 50% on the outside. The assembly was weighed periodically over 21 days to monitor water vapor diffusion through the multilayer until a constant value of the WVTR was measured according to equation (5).

$$WVTR = \frac{weigh\ loss\ (g)}{A_{film}\ (m^2)\cdot t\ (day)} \tag{5}$$

3 Results and Discussion

3.1 Characterization of the multilayers

In this study, PE/EVOH/PE and Ecovio/G-Polymer/Ecovio multilayer films are analyzed before and after hot stretching by means of a uniaxial tensile tester (i), gravity (ii) and a vacuum thermoformer (iii), to investigate the impact of maximal thinning on the final functionality of both multilayers.

Both films confer a high oxygen barrier due to the middle layer, which is composed of EVOH (ethylene vinyl alcohol copolymer) or G-Polymer (a water-soluble and biodegradable vinyl alcohol copolymer) [16]. The EVOH layer has an average thickness of 7.8 ± 1.0 µm and is flanked by adhesive and polyethylene layers, resulting in a total film thickness of 85.8 ± 0.5 µm. The G-Polymer layer (4.6 ± 0.2 µm) is flanked by 4-µm tie-layers and Ecovio® layers, giving a total film thickness of 82.0 ± 1.3 µm. Ecovio® is a commercial blend composed of 45% wt. poly(lactide acid) (PLA) and 55% wt. poly(butylene adipate-co-terephthalate) (PBAT), often applied in compostable packaging solutions, paper lining, shrink and transparent film, as well as thermoformed products.

First, the tensile properties of both multilayers are compared at room temperature (**Table 2**). Uniaxial stretching until break reveals higher stress, force and elongation at break (%) for the EVOH multilayer than the G-Pol multilayer. In addition, the difference between stretching in machine (MD) vs. cross direction (CD) is more pronounced in the Eco/G-Pol/Eco film.

Table 2: Tensile properties at break (n=5) at 23°C

23°C	**PE/EVOH/PE**		**Eco/G-Pol/Eco**	
	MD	**CD**	**MD**	**CD**
Stress (MPa)	25 ± 2	19 ± 2	19 ± 1	13 ± 1
Force (N)	31 ± 2	23 ± 2	22 ± 1	16 ± 1
Elongation (%)	707 ± 42	763 ± 204	235 ± 18	473 ± 83

Tensile stretching at elevated temperatures confirms the difference in MD and CD (**Figure 2**). Based on these data the maximal force and maximal elongation is defined for each multilayer. Of course, the films cannot be thinned until break, therefore the process is further optimized to obtain stretched films with thinned, but intact layers (validated by microscopic imaging).

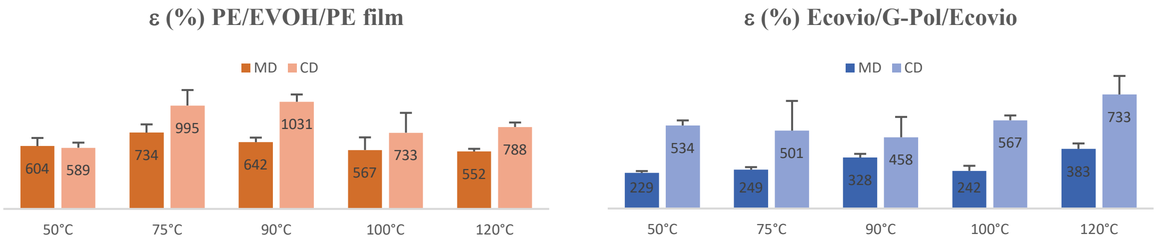

Figure 2: Tensile testing at elevated temperatures: elongation at break (ε, %).

It is generally known that G-Polymer and EVOH are sensitive to high relative humidity. In this study, the OTR of the original films is measured at 50% RH (in)/50% RH (out) and at 90% RH (in)/50% RH (out). The far higher moisture sensitivity of G-Polymer is clear from **Table 3**. For convenience, the oxygen permeability coefficient (PO_2) is calculated by normalizing the difference in thickness of the oxygen barrier layers. Based on these data, the EVOH film performs better at high RH, whereas the biofilm performs best in dryer conditions.

Table 3: OTR and PO_2 of both multilayers measured in different conditions of relative humidity

23°C **RH (in) / RH (out)**	**OTR** **cc/[m^2·day·atm]**		**PO_2** **cc·5 µm barrier layer/[m^2·day·atm]**	
	PE/EVOH/PE	**Eco/G-Pol/Eco**	**PE/EVOH/PE**	**Eco/G-Pol/Eco**
50% / 50% RH	1.76 ± 0.02	0.065	2.76 ± 0.03	0.060
90% / 50% RH	4.93 ± 0.41	10.26 ± 0.56	7.69 ± 0.63	9.43 ± 0.51

3.2 Hot stretching using gravity

During thermoforming, thinning and stretching of the film can occur either in MD, CD, biaxial or another combination thereof, depending on the location. Therefore, four approaches were hypothesized to simulate the thermoforming process on lab scale using gravity (2.3.1). The stretching operations are shown in **Figure 3**.

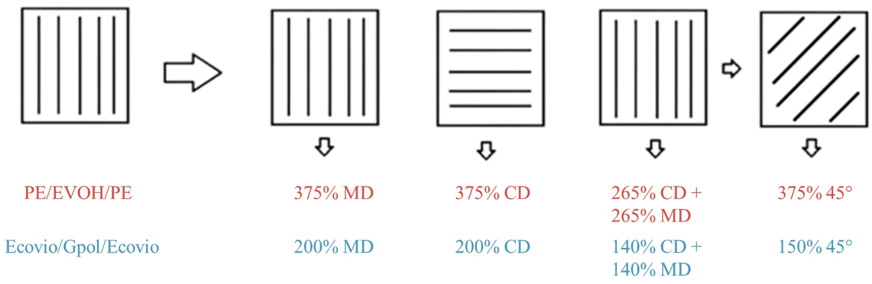

Figure 3: Four different hot stretching operations applied on the two multilayers.

3.2.1 Impact on the thickness of the film layers

The maximal strain (%) is determined by the condition where the film can be consecutively stretched in CD and MD direction without breaking. This strain is different for both multilayer films. During two-step stretching, a 70 mm x 60 mm-film is first stretched in CD direction (distance between the clamps is 40 mm), then the film is taken out, turned 90°, cut to a 70 mm x 40 mm-film and placed back between the clamps to be stretched in MD direction. In theory, the formula: $(265\%)^2 + (265\%)^2 = (375\%)^2$ can be used to calculate the final strain on the PE/EVOH/PE film. To compare the effect of this consecutive stretch, other film samples are stretched 375% in MD only, as well as 375% in CD only. Lastly, a film sample is turned 45°, a 70 mm x 60 mm-sample is cut and stretched, and thus the biaxial effect can be measured in theory. The Eco/G-Pol/Eco film can be stretched 140% in CD and 140% in MD, consecutively, without breaking. At higher strains, the film tears due to being stretched too hard. The formula: $(140\%)^2 + (140\%)^2 = (200\%)^2$, is used to determine the strain in MD and in CD direction. In addition, the 45° sample is stretched until 150%, because 200% resulted in micro tears, visual in optical microscopy.

After optimization, both multilayer films are stretched in duplicate in the oven using the four different stretching operations (**Figure 3**). Subsequently, the intactness and thickness of the different layers in the stretched films are evaluated microscopically. Representative microscopic images of the original and stretched PE/EVOH/PE films and eco/G-Pol/eco films are shown in **Figure 4** and **Figure 5** respectively. The average total and barrier layer thickness and % thinning of the EVOH and G-Pol multilayers are shown in **Table 4** and **Table 5**, respectively.

The consecutive stretching in CD and MD causes the greatest thinning of both films while the barrier layers remain intact and thinned equally. The EVOH multilayer is ~69% thinned in total, with an average EVOH layer thickness of ~2.1 µm. The G-Pol multilayer is ~82% thinned in total, with an average G-Pol layer thickness of ~1.2 µm.


Original film | MD stretch | CD stretch | CD+MD stretch | 45° stretch

Figure 4: Microscopical images of original and stretched PE/EVOH/PE films.

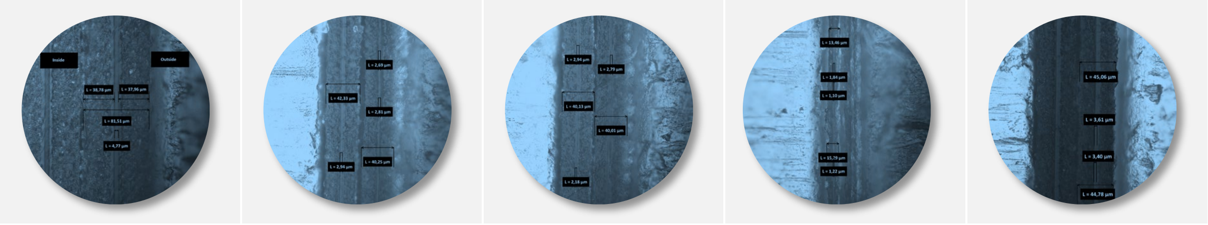
Original film | MD stretch | CD stretch | CD+MD stretch | 45° stretch

Figure 5: Microscopical images of original and stretched Eco/G-Pol/Eco films.

3.2.2 Impact on the oxygen barrier of the multilayers

The OTR of the stretched films is measured at high RH (90% inside/50% outside, 23°C). Despite a significant reduction in total film thickness (51-59%) and barrier layer thickness (44-56%), the OTR of the MD, CD and 45° stretched films is lower than the OTR of the original PE/EVOH/PE film (**Table 4**). This means that the thinned EVOH films exhibit improved oxygen barrier properties compared to the original film. The reduced sorption and diffusion of oxygen is most pronounced in the 45° samples and can be explained by reorientation, closer chain packaging, and restriction of chain mobility of polymer chains in the amorphous zones during stretching of the material [17]. However, this effect is limited, as exemplified by the consecutively stretched films in CD and MD, resulting in a quadrupled increase in OTR.

Table 4: Total and barrier layer thickness and OTR before and after stretching the PE/EVOH/PE multilayer

PE/EVOH/PE	**total film thickness**	**% thinning**	**barrier layer thickness**	**% thinning**	**OTR* cc/[m^2·day·atm]**	**OTR ▲▼**
Original film	**85.8 ± 0.5 µm**		**7.8 ± 1.0 µm**		**4.93 ± 0.41**	
MD stretching	35.1 ± 1.1 µm	59%	3.4 ± 0.4 µm	56%	4.27	▼
CD stretching	36.7 ± 6.9 µm	57%	4.4 ± 0.3 µm	44%	3.26	▼
CD+MD stretching	26.6 ± 0.2 µm	69%	2.1 ± 0.1 µm	73%	19.5	▲
45° stretching	41.8 ± 0.3 µm	51%	3.9 ± 0.1 µm	50%	2.58	▼

*90% RH (in)/50% RH (out), 23°C

Hot stretching of the Eco/G-Pol/Eco multilayer only results in a lower OTR in the case of the 45° stretched film (**Table 5**). However, when considering the PO_2 by normalizing the thickness of the (remaining) G-Pol layer, we show that de oxygen barrier of the MD (*4.9 cc·5 µm/m^2·day·atm*) and 45° (*6.0 cc·5 µm/m^2·day·atm*) stretched films is better than the original film (*9.4 cc·5 µm/m^2·day·atm*). The pronounced difference in MD and CD (**Table 2**) is also observed here, with a PO_2 of *10.7 cc·5 µm/m^2·day·atm*, for the CD stretched film, and similar to the EVOH film, consecutively stretching in CD and MD diminishes the oxygen barrier strongly to *25.1 cc·5 µm/m^2·day·atm*.

Table 5: Total and barrier layer thickness and OTR before and after stretching the Eco/G-Pol/Eco multilayer

Eco/G-Pol/Eco	**total film thickness**	**% thinning**	**barrier layer thickness**	**% thinning**	**OTR cc/[m^2·day·atm]**	**OTR ▲▼**
Original film	**82.0 ± 1.3 µm**		**4.6 ± 0.2 µm**		**10.26 ± 0.56**	
MD stretching	38.7 ± 3.0 µm	53%	2.3 ± 0.4 µm	50%	10.70	▲
CD stretching	37.4 ± 5.8 µm	54%	2.9 ± 0.5 µm	37%	18.43	▲
CD+MD stretching	14.4 ± 1.1 µm	82%	1.2 ± 0.1 µm	74%	104.6	▲
45° stretching	44.9 ± 0.2 µm	45%	3.5 ± 0.1 µm	24%	8.54	▼

*90% RH (in)/50% RH (out), 23°C

We conclude that the moisture sensitivity of the G-Pol multilayer makes it a less good candidate to be used at high RH. In addition, stretching during thermoforming can result in better oxygen gas barrier properties (especially when using EVOH), which is very positive, both from a functionality and sustainability point of view.

3.2.3 Impact on the water vapor permeability of the multilayers

Although stretching has a positive effect on the OTR of the EVOH multilayer, thinning of the film and its PE-layers negatively affects the water vapor barrier, as demonstrated in **Table 6**. Upon 51 to 59% thinning of the multilayer, the WVTR is 3.0 to 3.4 times increased.

The same effect is observed in the G-Pol multilayer with Ecovio-layers. Here, 45-54% thinning of the multilayer results in a 2.4 to 3.4-fold increase of the WVTR, as shown in **Table 7**.

Table 6: Total film thickness and WVTR before and after stretching the PE/EVO/PE multilayer

PE/EVOH/PE	**total film thickness**	**% thinning**	**WVTR* g/[m^2·day]**	**WVTR ▲▼**
Original film	**85.8 ± 0.5 µm**		**0.85 ± 0.01**	
MD stretching	35.1 ± 1.1 µm	59%	2.91	▲
CD stretching	36.7 ± 6.9 µm	57%	2.91	▲
CD+MD stretching	26.6 ± 0.2 µm	69%	/	
45° stretching	41.8 ± 0.3 µm	51%	2.52	▲

*0% RH (in)/50% RH (out), 23°C

Table 7: Total film thickness and WVTR before and after stretching the Eco/G-Pol/Eco multilayer

Eco/G-Pol/Eco	**total film thickness**	**% thinning**	**WVTR* g/[m^2·day]**	**WVTR ▲▼**
Original film	**82.0 ± 1.3 µm**		**2.19 ± 0.08**	
MD stretch	38.7 ± 3.0 µm	53%	7.10	▲
CD stretch	37.4 ± 5.8 µm	54%	8.17	▲
CD+MD stretch	14.4 ± 1.1 µm	82%	/	
45° stretch	44.9 ± 0.2 µm	45%	5.33	▲

*0% RH (in)/50% RH (out), 23°C

It must be noticed that the WVTR of the PE/EVOH/PE multilayer (0.85 ± 0.01 g/[m^2·day]) is lower than the WVTR of the Eco/G-Pol/Eco multilayer (2.19 ± 0.08 g/[m^2·day]). Indeed, the moisture sensitivity of the G-Pol multilayer is clearly observed in test conditions with 0% RH inside and 50% RH outside. At a smaller gradient (0% RH (in)/37% RH (out)), the WVTR of the G-Pol multilayer is 1.31 ± 0.14 g/[m^2·day], whereas at a higher moisture gradient (0% RH (in)/90% RH (out)) it becomes 17.9 ± 1.8 g/[m^2·day].

The water cup test is used to compare both multilayers in even higher moisture conditions (100% RH (in)/50% RH (out)). The results indicate a WVTR of 1.5 ± 0.2 g/[m^2·day] for the EVOH multilayer vs. 41.0 ± 3.0 g/[m^2·day] for the G-Pol multilayer. While the WVTR of the EVOH film does not even double compared to the WVTR at 0% RH (in)/50% RH (out), the WVTR of the G-Pol films increases ~19 times in these conditions.

It is concluded that thinning during thermoforming results in partial loss of the water vapor barrier. Again, the G-Pol multilayer suffers most under conditions of high RH.

3.3 Vacuum thermoforming on lab scale

Another approach to evaluate material thickness in function of functionality prior to industrial thermoforming is by using a lab scale vacuum thermoformer. To this end, different moulds were designed. The multilayer films are heated and vacuum formed resulting in thinned and stretched material in the bottom, walls and corners of the tray.

3.3.1 Impact on the thickness in different locations of the tray

The thermoformed trays are analysed for thickness in the different locations in accordance with the methodology described in Buntinx et al. [9]. The % thinning compared to the original film is calculated and visualised as shown for the PE/EVOH/PE tray B in **Figure 6**. The % thinning vary between 11-48%, 2-72%, 15-76% and 13-84% for tray type A, B, C and D, respectively (**Table 1**). The highest % thinning is associated with the deep drawn depth. The material is most thinned in the corners. The remaining thickness of the total and individual layers in the most critical locations are in line with the hot stretching data. E.g., the thinnest location in the G-Pol tray type A is 41 µm and 19 µm in tray type C. Similarly, the thinnest location was 24 µm in the EVOH tray type B. With the mould design type D, the multilayer could be deep drawn until 6 cm, however, the gas permeability properties of this tray could not be measured using the MOCONs because the sensor signal was above the threshold detection, indicating the limits for thinning of the ~80 µm multilayers.

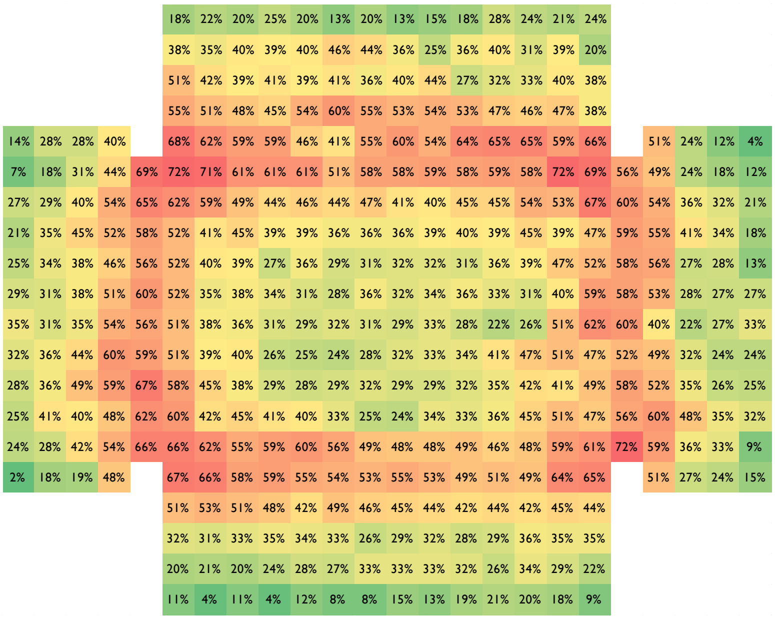

					18%	22%	20%	25%	20%	13%	20%	13%	15%	18%	28%	24%	21%	24%					
					38%	35%	40%	39%	40%	46%	44%	36%	25%	36%	40%	31%	39%	20%					
					51%	42%	39%	41%	39%	41%	36%	40%	44%	27%	32%	33%	40%	38%					
					55%	51%	48%	45%	54%	60%	55%	53%	54%	53%	47%	46%	47%	38%					
14%	28%	28%	40%		68%	62%	59%	59%	46%	41%	55%	60%	54%	64%	65%	65%	59%	66%		51%	24%	12%	4%
7%	18%	31%	44%	69%	72%	71%	61%	61%	61%	51%	58%	58%	59%	58%	59%	58%	72%	69%	56%	49%	24%	18%	12%
27%	29%	40%	54%	65%	62%	59%	49%	44%	46%	44%	47%	41%	40%	45%	45%	54%	53%	67%	60%	54%	36%	32%	21%
21%	35%	45%	52%	58%	52%	41%	45%	39%	39%	36%	36%	36%	39%	40%	39%	45%	39%	47%	59%	55%	41%	34%	18%
25%	34%	38%	46%	56%	52%	40%	39%	27%	36%	29%	31%	32%	32%	31%	36%	39%	47%	52%	58%	56%	27%	28%	13%
29%	31%	38%	51%	60%	52%	35%	38%	34%	31%	28%	36%	32%	34%	36%	33%	31%	40%	59%	58%	53%	28%	27%	27%
35%	31%	35%	54%	56%	51%	38%	36%	31%	29%	32%	31%	29%	33%	28%	22%	26%	51%	62%	60%	40%	22%	27%	33%
32%	36%	44%	60%	59%	51%	39%	40%	26%	25%	24%	28%	32%	33%	34%	41%	47%	51%	47%	52%	49%	32%	24%	24%
28%	36%	49%	59%	67%	58%	45%	38%	29%	28%	29%	32%	29%	29%	32%	35%	42%	41%	49%	58%	52%	35%	26%	25%
25%	41%	40%	48%	62%	60%	42%	45%	41%	40%	33%	25%	24%	34%	33%	36%	45%	51%	47%	56%	60%	48%	35%	32%
24%	28%	42%	54%	66%	66%	62%	55%	59%	60%	56%	49%	48%	48%	49%	46%	48%	59%	61%	72%	59%	36%	33%	9%
2%	18%	19%	48%		67%	66%	58%	59%	55%	54%	53%	55%	53%	49%	51%	49%	64%	65%		51%	27%	24%	15%
					51%	53%	51%	48%	42%	49%	46%	45%	44%	42%	44%	42%	45%	44%					
					32%	31%	33%	35%	34%	33%	26%	29%	32%	28%	29%	36%	35%	35%					
					20%	21%	20%	24%	28%	27%	33%	33%	33%	32%	26%	34%	29%	22%					
					11%	4%	11%	4%	12%	8%	8%	15%	13%	19%	21%	20%	18%	9%					

Figure 6: Visual representation of % thinning in different locations of a PE/EVOH/PE tray type B.

3.3.2 Impact on the oxygen barrier of the trays

When considering trays, the OTR is measured in cc/[package·day·atm]). By dividing this OTR by the tray surface (**Table 1**), the OTR of the trays can be expressed in cc/[m²·day·atm] and compared with the OTR of the film. From the data in **Table 8**, it is clear that the G-Pol tray and film have a 10 to 27-fold better oxygen barrier in drier conditions then the EVOH material (50% RH (in)/50% RH (out)). But similar as in the hot gravity stretching, the OTR of the G-Pol trays does not improve due to the processing step. In contrast, when using EVOH multilayer, a clear improvement in the OTR after thermoforming the multilayer can be observed, in line with the gravity method.

Table 8: OTR of films and trays expressed in the same units

	PE/EVOH/PE		Eco/G-Pol/Eco	
OTR	**cc/[m^2·day·atm]**	▲▼	**cc/[m^2·day·atm]**	▲▼
Original film*	4.93 ± 0.41		10.26 ± 0.56	
Original film**	**1.76 ± 0.02**		**0.065**	
Tray type A			0.10	▲
Tray type B	1.36 ± 0.05	▼	0.14± 0.01	▲
Tray type C			0.16	▲

*90% RH (in)/50% RH (out), 23°C; **50% RH (in)/50% RH (out), 23°C

3.3.3 Impact on the water vapour barrier of the trays

A similar approach is used to calculate the WVTR of the trays in g/[m^2·day]. Table 9 shows that de WVTR of the tray increases after thermoforming, which is expected.

Again, the moisture sensitivity plays a key role, with the G-Pol tray showing almost comparable water vapor barrier properties compared to the EVOH tray in drier conditions (0% RH (in)/25% RH (out)).

Table 9: WVTR of films and trays expressed in the same units

	PE/EVOH/PE		**Eco/G-Pol/Eco**	
WVTR	**g/[m^2·day]**	▲ ▼	**g/[m^2·day]**	▲ ▼
Original film*	**0.85 ± 0.01**		**2.19 ± 0.08**	
Tray type B	1.81 ± 0.26	▲	> detection limit	▲
Tray type B**	0.79		0.98	

*0% RH (in)/50% RH (out), 23°C; **0% RH (in)/25% RH (out), 23°C

4 Conclusions

This study has demonstrated two lab scale approaches to investigate the maximal thinning of multilayer films and their associated effects on the final properties of thermoformed packaging. Both hot stretching using gravity and lab scale thermoforming can reveal the limits of material thinning and stretching based on qualitative and quantitative data. Such strategies become essential in the search for sustainable packaging materials.

Our study stresses the importance of selecting correct test conditions, such as % RH and temperature, during the evaluation of materials. The product to be packaged should be considered from the start. From the comparison of the commercial PE/EVOH/PE and Ecovio®/G-polymer/Ecovio multilayers, we show that the use of G-Pol is preferred in dry conditions, as very high oxygen barrier properties are achieved. EVOH is less sensitive to relative humidity as compared to G-Pol, being the preferred material for packaging high(er) moisture food products.

The G-Pol multilayer can be combined with other biodegradable materials, for example in paper lining, creating environmentally friendly packaging that can be disposed of together with food waste via organic recycling.

In accordance with Ceflex and RecyClass guidelines, multilayers containing EVOH up to 5% of the total weight of the PE film, can be recycled in current polyolefin recycling streams, offering a suitable end-of-life solution.

Finally, although the material is thinned during thermoforming, this effect is (partly) neutralized by reorientation of the polymer chains of the barrier material. This positive effect on the oxygen barrier is very pronounced in the PE/EVOH/PE multilayer and allows to use less EVOH, which makes the multilayer better recyclable.

Acknowledgements

The authors express special appreciation to all people involved in this project for their constructive feedback during the study. The authors also acknowledge Tom De Weyer (MakerSpace UHasselt) and Wouter Marchal (Analytical & Circular Chemistry, imo-imomec, UHasselt) for access to the thermoformer and DSC, respectively.

References

1. C. Y. Barlow and D. C. Morgan, *Polymer film packaging for food: An environmental assessment.* Resources, Conservation and Recycling, 2013. **78**: p. 74-80.
2. Anna Sophia Bauer, et al., *Recyclability and redesign challenges in multilayer flexible food packaging—a review.* Foods, 2021. **10**(11): p. 2702.
3. Eurostat.EU packaging waste generation with record increase.2023.Available from: https://ec.europa.eu/eurostat/web/products-eurostat-news/w/ddn-20231019-1
4. European Commission.Proposal for a Regulation of the European and of the Council on packaging and packaging waste, amending Regulation (EU) 2019/1020 and Directive (EU) 2019/904, and repealing Directive 94/62/EC.2022.Available from: https://eur-lex.europa.eu/legal-content/EN/TXT/HTML/?uri=CELEX:52022PC0677
5. Martina Seier, et al., *Prospects for Recyclable Multilayer Packaging: A Case Study.* Polymers, 2023. **15**(13): p. 2966.
6. RecyClass. PE flexible films recycling: new findings for functional barriers. 2019; Available from: https://recyclass.eu/news/pe-flexible-films-recycling-new-findings-for-functional-barriers/.
7. Camila Távora de Mello Soares, et al., *Recycling of multi-material multilayer plastic packaging: Current trends and future scenarios.* Resources, conservation and recycling, 2022. **176**: p. 105905.
8. Florencia Versino, et al., *Sustainable and Bio-Based Food Packaging: A Review on Past and Current Design Innovations.* Foods, 2023. **12**(5).
9. Mieke Buntinx, et al., *Evaluation of the Thickness and Oxygen Transmission Rate before and after Thermoforming Mono- and Multi-layer Sheets into Trays with Variable Depth.* Polymers, 2014. **6**(12): p. 3019-3043.
10. Griet Knockaert, et al., *Thickness and Gas Permeability Properties of PLA and PLA/EVOH/PLA before and after Thermoforming into Variable Tray Types.* 28th IAPRI Symposium on Packaging hosted by the School of Engineering and Management Vaud (HEIG-VD) and Nestle Research, 2017.
11. Siti Munirah Saharin, et al., *Effect of OH Segmental Length on the Iodine Complex Formation of Ethylene–Vinyl Alcohol Random Copolymers.* Macromolecules, 2015. **48**(24): p. 8867-8876.
12. ASTM International, *ASTM F1927 Standard Test Method for Determination of Oxygen Gas Transmission Rate, Permeability and Permeance at Controlled Relative Humidity Through Barrier Materials Using a Coulometric Detector.* 2007: West Conshohocken, PA.
13. ASTM International, *ASTM F1307 Standard Test Method for Oxygen Transmission Rate Through Dry Packages Using a Coulometric Sensor.* 2007: West Conshohocken, PA.
14. ASTM International, *ASTM F1249. Standard Test Method for Water Vapor Transmission Rate Through Plastic Film and Sheeting Using a Modulated Infrared Sensor.* 2007: West Conshohocken, PA.
15. ASTM E-96, *Standard Test Methods for Water Vapor Transmission of Materials*. 2017.
16. Mitsubishi Chemical Corporation. Nichigo G-PolymerTM. [cited 2024 March]; Available from: https://soarus.com/product/nichigo-g-polymer/.
17. Ahmed Makradi, et al., *Thermoforming process of semicrystalline polymeric sheets: Modeling and finite element simulations.* Polymer Science Series A, 2008. **50**(5): p. 550-557.